



## A numerical approach to non-Fourier heat transfer in liver tumor during laser irradiation

Mohsen Balavand, Iman Eltejaei, Afsaneh Mojra\*

Department of Mechanical Engineering, K. N. Toosi University of Technology, Tehran, Iran

**ABSTRACT:** Thermal therapy is a type of cancer treatment that uses heat to kill cancer cells, but it also may harm healthy tissue. Numerical simulations can help to accurately analyze the thermal damage of the tissue during heat exposure. The target of this study is to investigate the effect of time lags on the thermal response of the biological tissue during laser irradiation to the tumoral tissue. The classical Fourier, single phase lag (SPL) and dual phase lag (DPL) models of bio-heat transfer are implemented and compared. The numerical solution based on the finite volume method (FVM) is applied to solve the bio-heat transfer equations. Beer-Lambert's law is applied to determine the heat source distribution caused by the laser irradiation. The thermal damage caused by the laser exposure for the three models is discussed. Results show that the DPL model predicts a significantly different thermal damage from the classical Fourier and the SPL models. It is observed that the DPL model predicts the maximum temperature 4.1 °C and 5.7 °C less than the Fourier and the SPL models, respectively. The deviation between the maximum temperatures obtained by the three models can be attributed to the finite speed of thermal wave propagation in the non-Fourier models.

### Review History:

Received: May, 15, 2020  
Revised: Jun. 12, 2020  
Accepted: Jun. 12, 2020  
Available Online: Dec. 01, 2020

### Keywords:

Biological tissue  
Bio-heat transfer  
Beer-Lambert's law  
Finite volume method  
Thermal damage.

## 1- INTRODUCTION

The thermal therapy is regarded as a type of the cancer treatment in which the biological tissue is exposed to a heat source with a high temperature [1], and it is often combined with other types of cancer treatment methods to improve the efficiency of the therapies. It is essential to estimate the temperature distribution to maximize the destruction of the cancerous tissue while minimize the damage to the surrounding healthy cells. To estimate the heat transfer in biological tissues, the Pennes bio-heat transfer equation (PBHE) is conventionally used [2]. The PBHE model is based on the Fourier's law which depicts an infinite speed of the thermal wave propagation. This assumption provides unsatisfactory results since the biological tissues have a non-homogeneous structure, which results to a time lag for the heat to propagate in the tissue [3]. This issue has been considered by Cattaneo [4] and Vernotte [5] by proposing a single-phase lag (SPL) heat conduction model which considers the time lag between the temperature gradient and the heat flux. In continuation to the SPL model, Tzou [6] introduced a dual-phase lag model (DPL) model by adding a second phase lag to the heat transfer equation. In this model, the phase lags are named as  $\tau_q$  and  $\tau_T$ , where  $\tau_q$  is the time delay for the heat flux propagation and  $\tau_T$  is the lag time for the occurrence of the temperature variation. The DPL model is able to capture

the micro-scale response of the tissue in both time and space.

The SPL model was used by Jaunich et al. [7] to analyze the temperature distribution in the biological tissue when it is exposed to the laser irradiation. The result showed that the SPL heat conduction model is a more accurate model than the PBHT model. Zhou et al. [8] used the SPL model of bio-heat transfer to investigate the thermal damage caused by the laser irradiation in the biological tissue. The result indicated that the threshold of laser energy at which an irreversible damage is occurred is 50% higher when the non-Fourier effect is not included.

Zhang et al. [9] developed a numerical method to solve the DPL model during the pulsed laser heating of the skin tissue. They concluded that in the non-Fourier heat conduction, unlike the Fourier heat conduction, the temperature rises nonlinearly. McDonough et al. [10] developed a numerical method for solving the DPL equation and results depicted that the estimation by the DPL model is in a better agreement with the experimental results compared to the classical Fourier heat equation. Askarizadeh et al. [11] established an analytical solution of the DPL bio-heat transfer equation in the skin tissue. They showed that it is important to use the DPL model specially to predict the thermal damage to the skin. Kumar et al. [12] studied the heat transfer problem in a biological tissue and they obtained the exact solution for the classical Fourier, the SPL and the DPL models. They concluded that the DPL model is more consistent with the experimental data. Lin et al.

\*Corresponding author's email: mojra@kntu.ac.ir





$$\left(1 + \tau_q \frac{\partial}{\partial t}\right) q(X, t) = -\left(1 + \tau_T \frac{\partial}{\partial t}\right) k \nabla^2 T(X, t) \quad (4)$$

The dual-phase lag constitutive equation (Eq. (4)) in combination with the energy balance equation (Eq. (1)), results in Eq. (5):

$$\left(1 + \tau_T \frac{\partial}{\partial t}\right) k \nabla^2 T = \left(1 + \tau_q \frac{\partial}{\partial t}\right) \left[ \rho c \frac{\partial T}{\partial t} - \rho_b c_b \omega_b (T_b - T) - Q_m - Q_r \right] \quad (5)$$

Eq. (5) is known as the DPL bio-heat transfer equation. In this equation, similar to the PBHT equation, blood perfusion rate and metabolic heat generation have been considered to account for the live biological tissue. Consequently, the values of phase lags are derived for the live tissue conditions.

The external heat source in Eq. (5) is determined by the Beer-Lambert's law which calculates the distribution of laser radiation on the biological tissue. The Beer-Lambert law assumes that the incident laser beam completely propagates in a single direction. The heat source distribution in depth (y) using Beer-Lambert's law could be computed as Eq. (6).

$$Q_r(y) = \mu_a I_0(\lambda) \exp\left[-(\mu_a + \mu'_s)y\right] \quad (6)$$

Where,  $\lambda$  and  $I_0(\lambda)$  are the wavelength and the incident intensity of the laser respectively. The wavelength of the laser is considered  $\lambda = 1064$  nm.  $\mu_a$  is the absorption coefficient,  $\mu'_s$  is the reduced scattering coefficient which is expressed as  $\mu'_s = \mu_s(1 - g)$  where,  $\mu_s$  denotes the scattering coefficient and  $g$  is the anisotropy factor.  $y$  is the depth normal to the tissue surface.

### 2.2. Thermal damage estimation

The irreversible thermal damage is calculated using the Arrhenius equation. The damage parameter  $\Omega$  is expressed by Eq. (7) [15]:

$$\Omega = A \int_0^t \exp\left(\frac{-E_a}{RT(t)}\right) dt \quad (7)$$

Where  $A$ ,  $E_a$  and  $R$  stand for the frequency factor, the activation energy of denaturation reaction and the universal gas constant which equals to  $8.314 \text{ J.mol}^{-1}\text{K}^{-1}$ , respectively.

$T(t)$  is the tissue temperature over the time and  $t$  is the time when the damage parameter  $\Omega$  is calculated.  $\Omega=1$  represents the permanent thermal damage to the tissue. In the present study, Arrhenius parameters of the tumor and the healthy liver tissue,  $E_a = 6.524 \times 10^5 \frac{\text{J}}{\text{mol.K}}$  and  $A = 2.68788 \times 10^{103} \text{ s}^{-1}$  are employed to evaluate the thermal damage [16].

### 2.3. Numerical method

The Finite Volume Method (FVM) is employed to solve the governing Eq. (5). The computational domain is divided to equal control volumes as illustrated in Fig. 1. A numerical code is developed to solve the discretized equations using the MATLAB software.

By applying central difference scheme in space and backward difference scheme in time, the discretized form of Eq. (5) can be expressed as follows:

$$\begin{aligned} -a_S T_S^{t+\Delta t} + a_P T_P^{t+\Delta t} - a_N T_N^{t+\Delta t} &= a_E T_E^{t+\Delta t} + a_W T_W^{t+\Delta t} + B \\ a_S = a_N &= \frac{k \Delta t \Delta x + k \tau_T \Delta x}{\Delta t \Delta y + \tau_q \Delta y} \\ a_E = a_W &= \frac{k \Delta t \Delta y + k \tau_T \Delta y}{\Delta t \Delta x + \tau_q \Delta x} \\ a_P &= a_E + a_W + a_N + a_S + \frac{\rho c \Delta x \Delta y}{\Delta t} + \rho_b \omega_b c_b \Delta x \Delta y \quad (8) \\ B &= \left( \frac{\rho c \Delta x \Delta y}{\Delta t} + \frac{2k \tau_T \Delta y}{\Delta t \Delta x + \tau_q \Delta x} + \frac{2k \tau_T \Delta x}{\Delta t \Delta y + \tau_q \Delta y} \right) \\ &T_P^t - \frac{k \tau_T \Delta y}{\Delta t \Delta x + \tau_q \Delta x} (T_E^t + T_W^t) \\ &- \frac{k \tau_T \Delta x}{\Delta t \Delta y + \tau_q \Delta y} (T_N^t + T_S^t) - r \Delta y (q_e^t - q_w^t) \\ &- r \Delta x (q_s^t - q_n^t) + (Q_m + Q_r + \rho_b \omega_b c_b T_b) \Delta x \Delta y \\ r &= \frac{\tau_q}{\Delta t + \tau_q} \\ q_e^t - q_w^t &= -m T_E^t + 2m T_P^t - m T_W^t + \frac{k \tau_T}{\Delta t \Delta x + \tau_q \Delta x} \\ &(T_E^{t-\Delta t} - 2T_P^{t-\Delta t} + T_W^{t-\Delta t}) + r (q_e^{t-\Delta t} - q_w^{t-\Delta t}) \\ m &= \frac{k \Delta t + k \tau_T}{\Delta t \Delta x + \tau_q \Delta x} \end{aligned} \quad (9)$$

**Table 1. Mesh independence study**

	Number of elements			
	11220	15725	20000	22050
$T(0,0)$	73.67 °C	74.44 °C	75.1 °C	75.08 °C
Deviation from the finest grid size	1.88%	0.85%	0.02%	0

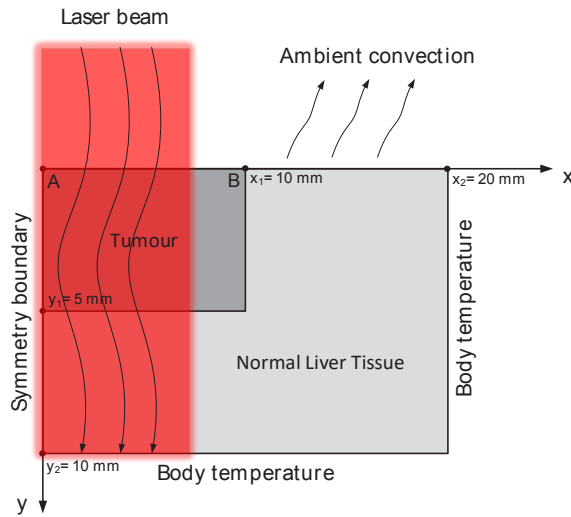


**Fig. 2. 2D axisymmetric geometry of the tissue**

**Table 2. Thermo-physical and optical properties of the liver tissue and the tumor [17, 18]**

Materials	Property							
	$\rho$ (kg/m <sup>3</sup> )	$c$ (J/(kg.K))	$k$ (W/(m.K))	$\omega_b$ (m <sup>3</sup> / (m <sup>3</sup> .s))	$\mu_a$ (cm <sup>-1</sup> )	$\mu_s$ (cm <sup>-1</sup> )	$g$	$\mu'_s$ (cm <sup>-1</sup> )
Liver tissue	1000	4200	0.5	$1 \times 10^{-3}$	2	152	0.948	7.9
Tumor	1100	4200	0.55	$9.1 \times 10^{-4}$	2.5	188	0.952	9

**Table 3. List of parameters used for the present study**

Parameter	Value	Parameter	Value
$R$ (J.mol <sup>-1</sup> .K <sup>-1</sup> )	8.314	$I_0$ (W/cm <sup>2</sup> )	4
$E_a$ (J.mol <sup>-1</sup> .K <sup>-1</sup> )	$6.524 \times 10^5$	$\lambda$ (nm)	1064
$A$ (s <sup>-1</sup> )	$2.68788 \times 10^{103}$	$\rho_b$ (kg/m <sup>3</sup> )	1000
$h_{conv}$ (W.m <sup>-2</sup> .K <sup>-1</sup> )	5	$C_b$ (J.kg <sup>-1</sup> .K <sup>-1</sup> )	3860
$T_\infty$ (°C)	25	$Q_m$ (W/m <sup>3</sup> )	1091
$T_{body}$ (°C)	37	$\tau_q$ (s)	5.66
$T_0$ (°C)	37	$\tau_T$ (s)	22

**Table 4. Verification of the numerical code**

Temperature	Location		
	y=0	y=2.5mm	y=5mm
The present study	73.35 °C	56.64 °C	46.08 °C
Soni et al. [17]	73.52 °C	57.15 °C	45.95 °C
Error	0.2%	0.9%	0.3%

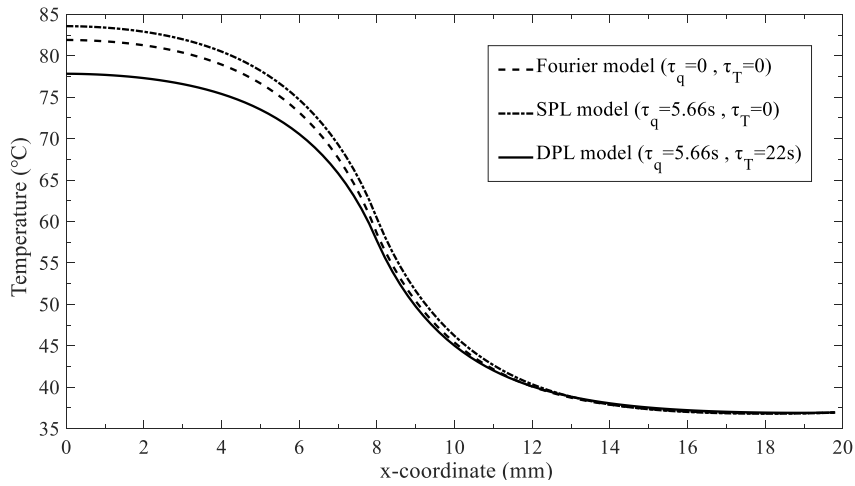


**Fig. 3. Temperature variation on line A-B for the Fourier, SPL and DPL models at 100 s of laser irradiation**

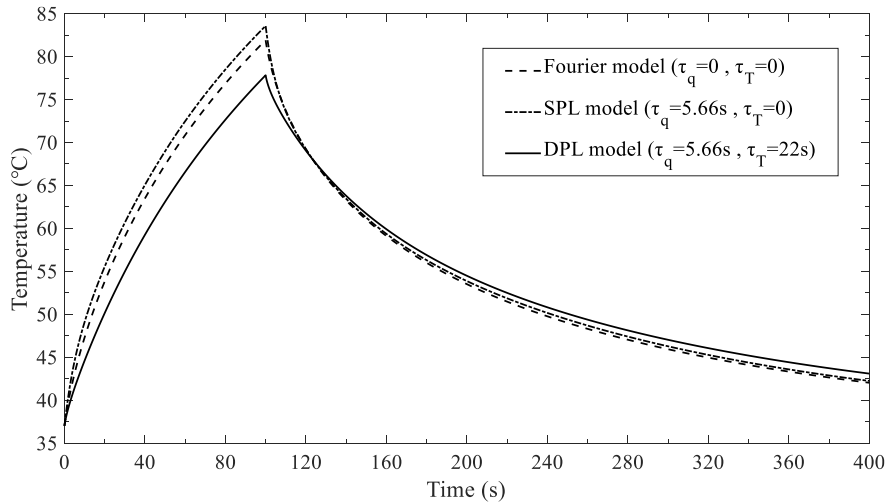


**Fig. 4. Temporal variation of temperature estimated by the Fourier, SPL and DPL models at point A**

$$q_n^t - q_s^t = -nT_N^t + 2nT_P^t - nT_S^t + \frac{k\tau_T}{\Delta t \Delta y + \tau_q \Delta y} \quad (10)$$

$$n = \frac{k\Delta t + k\tau_T}{\Delta t \Delta y + \tau_q \Delta y}$$

$$(T_N^{t-\Delta t} - 2T_P^{t-\Delta t} + T_S^{t-\Delta t}) + r(q_n^{t-\Delta t} - q_s^{t-\Delta t})$$

The resulting system of algebraic equations (Eqs. (8)-(10))

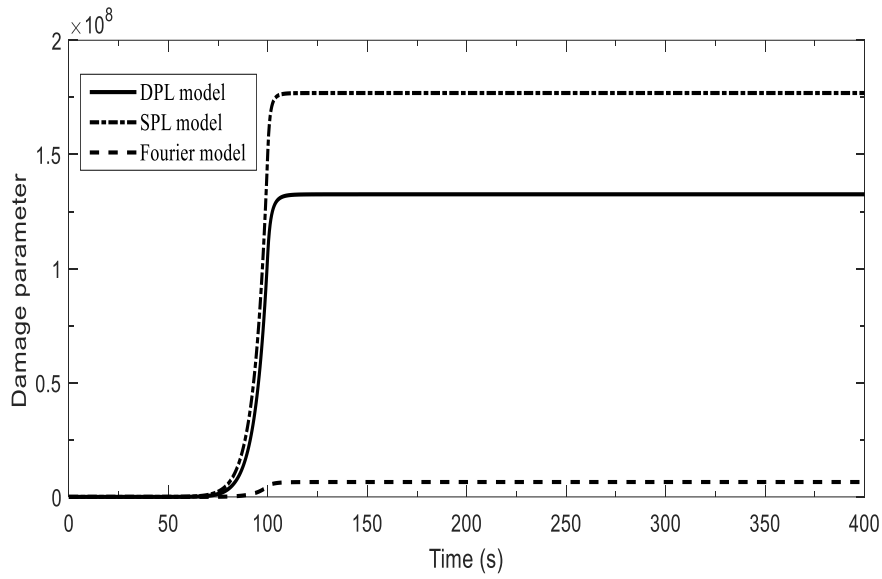


Fig. 5. Temporal evolution of thermal damage at point A obtained by the Fourier, SPL and DPL models

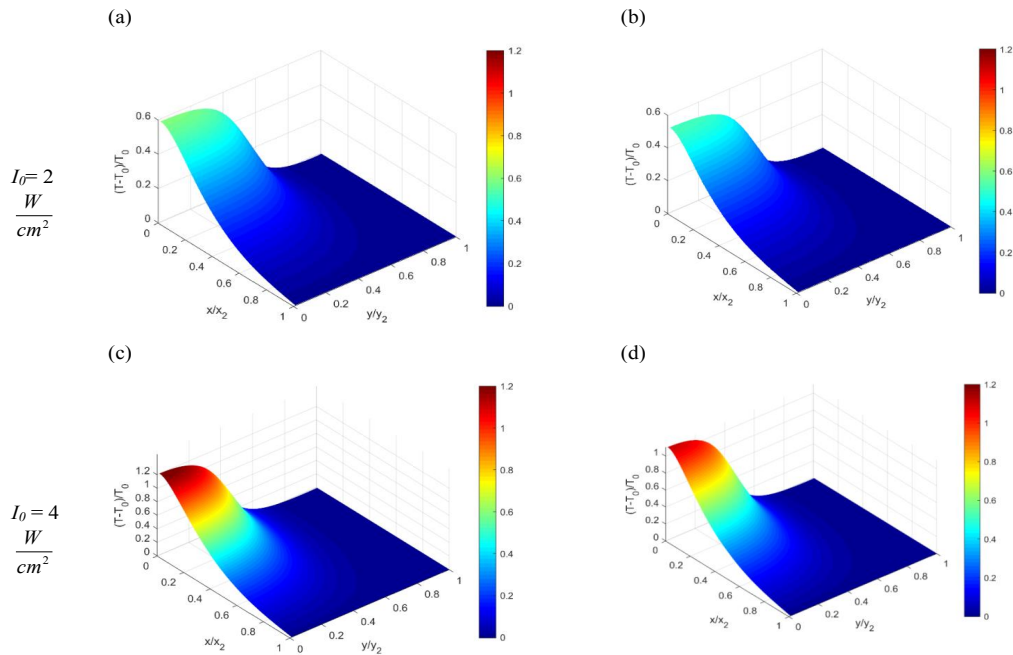


Fig. 6. The surface plot of the dimensionless temperature distribution in tumoral and healthy tissues with respect to the dimensionless spatial coordinates at different intensities for (a) & (c) the Fourier model and (b) and (d) the DPL model

is solved iteratively for temperature in each time step. The mesh independence study is presented in Table 1. This table provides the temperature at point (0,0), predicted by the DPL model for different grid sizes. It is observed that the deviation of the finest grid size and the case with 20000 elements is negligible. So, the grid with 20000 elements is regarded as the optimum value for the grid size. The time step is set to 0.01 based on the physics of the problem.

In this study, the DPL model is employed for analyzing the

heat conduction in a tumor of the liver tissue. The incident radiation beam is applied to the upper surface of the tissue for a period of 100s. The laser beam diameter is 16mm. A 2D axisymmetric computational domain is used to perform the numerical simulation. The geometry and the related dimensions are represented in Fig. 2. The thermo-physical and the optical properties of the liver tissue and the tumor are listed in Table 2. The convective heat transfer coefficient is  $h_{conv} = 5 \text{ W}/(\text{m}^2 \cdot \text{K})$ , the ambient temperature is  $T_{\infty} = 25 \text{ }^{\circ}\text{C}$ ,

**Table 5. Percentage of tumor necrosis**

Laser intensity $\frac{W}{cm^2}$	Bio-heat transfer models		
	Fourier model	SPL model ( $\tau_q = 5.66s$ )	DPL model ( $\tau_q = 5.66s$ & $\tau_T = 22s$ )
2	25.5%	29.0%	19.7%
3	51.8%	58.0%	45.7%
4	72.6%	81.0%	66.2%

the body temperature  $T_{body}=37$  °C and the initial temperature is  $T_0=37$  °C. Laser intensity is considered to be  $4\frac{W}{cm^2}$ . The blood density, the blood specific heat and the metabolic heat generation rate are  $1000\text{ kg/m}^3$ ,  $3860\text{ J/(kg.K)}$  and  $1091\text{ W/m}^3$ , respectively. Parameters of the study are reported in Table 3.

In order to verify the numerical analysis, the result of the present study is compared with the result of Soni et al. [17]. The value of temperature at  $x=0$  and different depths ( $y$ ) is given in Table 4. It is observed that the obtained values of temperature are in good agreement with those derived by Soni et al. [17], and the temperature deviation does not exceed 1%.

The initial and boundary conditions of the problem are defined in Eq. (11)-(15):

$$\text{At } x = 0 \text{ and } 0 \leq y \leq y_2; q(0, y, t) = 0 \tag{11}$$

$$\text{At } x = x_2 \text{ and } 0 \leq y \leq y_2; T(x_2, y, t) = T_{body} \tag{12}$$

$$\text{(13) At } y = y_2 \text{ and } 0 \leq x \leq x_2; T(x, y_2, t) = T_{body} \tag{13}$$

$$\text{At } y = 0 \text{ and } 0 \leq x \leq x_2; q(x, 0, t) = h_{conv}(T - T_\infty) \tag{14}$$

$$T(x, y, 0) = T_0, q(x, y, 0) = 0 \tag{15}$$

For the heat transfer modeling in biological tissue the following assumptions are made: (1) The value of the phase lags is assumed to be same for the normal tissue and the tumor; (2) it has been assumed that the right and the bottom boundaries of the model are maintained at constant temperature due to the thermoregulation process in the human body; (3) the tissue and the tumor have uniform and equal temperatures prior to the laser irradiation; (4) the metabolic heat generation and the blood perfusion rate are considered for the live tissue modeling; (5) the thermo-physical properties and the blood perfusion rate are assumed to be constant with temperature; (6) the propagation of incident laser beam is assumed to be unidirectional; (7) the tissue and the tumor are approximated as two-dimensional axisymmetric shapes.

### 3- RESULTS AND DISCUSSION

Li et al. [19] conducted experiments on the liver tissue and

determined the values of the thermal relaxation times which is used in the present study. The values of the time lags are set at  $\tau_q = 5.66s$  and  $\tau_T = 22s$  [19] for the DPL model and the phase lag of the heat flux for the SPL model is set at  $\tau_q = 5.66s$ . To investigate the effect of the thermal relaxation times during the laser exposure, the temperature profile for the three models (Fourier, SPL and DPL) by the end of the exposure time are compared. The temperature variation of the three models are plotted on path A-B (shown in Fig. 2), and is illustrated in Fig. 3. It can be observed that the peak value of temperature estimated by the DPL model is  $4.1$  °C and  $5.7$  °C less than the Fourier and the SPL model, respectively. As the distance from center line increases, temperature difference between the three models is reduced. It could be inferred that the importance of the lagging behavior becomes more significant at higher temperature gradients.

The thermal response of point A (shown in Fig. 2) is presented in Fig. 4. The slope of the temperature profile as it climbs upward in the SPL model is higher than other models which leads to a higher temperature estimation. Based on the experimental evidences [12], the DPL model estimates a more realistic temperature among the three models So, it could draw the conclusion that the temperature predicted by the SPL model is overestimated. In addition, it could be seen that in the decaying part of the temperature profile, the temperature decrease slowly in the DPL model. As expected, due to lagging behavior, it takes time to dissipate the heat.

Temporal evolution of the thermal damage at point A for the three models is presented in Fig. 5. According to this figure, the SPL model estimates the highest thermal damage compared to the other models. Meanwhile, the Fourier model estimates the lowest thermal damage because this model assumes an infinite speed of the thermal wave propagation. In the DPL model, there is a time delay for the heat transmission in the tissue, consequently the thermal damage estimated by the DPL model is higher than the Fourier model.

Surface plots of the dimensionless temperature distribution in the tumoral and healthy liver tissues with respect to the dimensionless spatial coordinates are shown in Fig. 6. In this figure, two different laser intensities are employed for the Fourier and DPL models. The investigation of this figure depicts that as the laser intensity increases, the temperature increases at the irradiated surface meanwhile the difference

between the two models is increased.

The percentage of tumor necrosis for the three models is presented in Table 5. From this table, the permanently damaged area obtained by the DPL model is much smaller than the Fourier and the SPL models. As the laser intensity increases, the effect of time lags on the permanently damaged area of the tissue becomes more important. This estimation is of significant importance in the clinical applications since it is required to have the maximum destruction of the tumoral tissue while the healthy tissue remains unaffected. As expected, results show that the SPL model overestimate the necrotic area. Therefore, considering the two-phase lags may lead to more accurate thermal damage estimation.

#### 4- CONCLUSIONS

An Accurate estimation of the thermal response in biological tissues subjected to the laser irradiation is necessary to increasing the efficiency of a treatment in the clinical application. Due to the non-homogeneous structure of biological tissues, the assumption of an infinite speed of the heat propagation is not applicable. The non-Fourier heat conduction models should be taken into account to justify the actual behavior of the tissue. In this study, a FVM-based 2D numerical code is employed to investigate the effect of the phase lags on the temperature profile in the liver tissue. The value of phase lags obtained by Li [19] is used for the simulation. It is observed that the two-phase lags have significant influence on the thermal damage and temperature distribution in the tumor and in the healthy tissue. By increasing the laser intensity, the effect of the phase lags on the temperature distribution is elaborated. The results show that the DPL model predicts a moderate thermal damage compared to other models. By considering the DPL model, the maximum temperature is decreased and consequently the extent of the necrotic tumor area is obviously reduced.

#### NOMENCLATURE

$A$	Frequency factor, $s^{-1}$
$c$	Specific heat of the tissue, $J/(kg.K)$
$E_a$	Activation energy of denaturation reaction, $J/(mol.K)$
$g$	Anisotropy factor
$h_{conv}$	Convective heat transfer coefficient, $W/(m^2.K)$
$I_0$	Incident intensity, $W/cm^2$
$k$	Thermal conductivity, $W/(m.K)$
$q$	Heat flux vector, $W/cm^2$
$Q_m$	Metabolic heat generation rate, $W/m^3$
$Q_r$	External environmental heat source term, $W/m^3$
$R$	Universal gas constant, $J/(mol.K)$
$T$	Local tissue temperature, $^{\circ}C$

$t$	Time, s
$T_0$	Ambient temperature, $^{\circ}C$
$X$	Position vector, m

#### GREEK SYMBOLS

$\mu_a$	Absorption coefficient, $cm^{-1}$
$\mu_s$	Scattering coefficient, $cm^{-1}$
$\mu'_s$	Reduced scattering coefficient, $cm^{-1}$
$\lambda$	Wavelength, nm
$\rho$	Density of the tissue, $kg/m^3$
$\tau_q$	Phase lag of the heat flux, s
$\tau_T$	Phase lag of the temperature gradient, s
$\Omega$	Damage parameter
$\omega_b$	Blood perfusion rate, $m^3/(m^3.s)$

#### SUBSCRIPT

$0$	Initial
$b$	Blood
$body$	Body core

#### REFERENCES

- [1] L. Lutgens, J. van der Zee, M. Pijls-Johannesma, D.F. De Haas-Kock, J. Buijsen, G.A. Mastrigt, G. Lammering, D.K. De Ruyscher, P. Lambin, Combined use of hyperthermia and radiation therapy for treating locally advanced cervical carcinoma, The Cochrane database of systematic reviews, (1) (2010) Cd006377.
- [2] H.H. Pennes, Analysis of Tissue and Arterial Blood Temperatures in the Resting Human Forearm, Journal of Applied Physiology, 85(1) (1998) 5-34.
- [3] W. Kaminski, Hyperbolic heat conduction equation for materials with a nonhomogeneous inner structure, Journal of Heat Transfer, 112(3) (1990) 555-560.
- [4] C. Cattaneo, A form of heat-conduction equations which eliminates the paradox of instantaneous propagation, Comptes Rendus, 247 (1958) 431.
- [5] P. Vernotte, Some possible complications in the phenomena of thermal conduction, Comptes Rendus, 252(1) (1961) 2190-2191.
- [6] D.Y. Tzou, A Unified Field Approach for Heat Conduction From Macro- to Micro-Scales, Journal of Heat Transfer, 117(1) (1995) 8-16.
- [7] M. Jaunich, S. Raje, K. Kim, K. Mitra, Z. Guo, Bio-heat transfer analysis during short pulse laser irradiation of tissues, International Journal of Heat and Mass Transfer, 51(23) (2008) 5511-5521.
- [8] J. Zhou, Y. Zhang, J.K. Chen, Non-Fourier Heat Conduction Effect on Laser-Induced Thermal Damage in Biological Tissues, Numerical Heat Transfer, Part A: Applications, 54(1) (2008) 1-19.
- [9] Y. Zhang, B. Chen, D. Li, Non-Fourier effect of laser-mediated thermal behaviors in bio-tissues: A numerical study by the dual-phase-lag model, International Journal

- of Heat and Mass Transfer, 108 (2017) 1428-1438.
- [10] J.M. McDonough, I. Kunadian, R.R. Kumar, T. Yang, An alternative discretization and solution procedure for the dual phase-lag equation, *Journal of Computational Physics*, 219(1) (2006) 163-171.
- [11] H. Askarizadeh, H. Ahmadikia, Analytical analysis of the dual-phase-lag model of bioheat transfer equation during transient heating of skin tissue, in, 2014.
- [12] D. Kumar, S. Singh, K. Rai, Analysis of Classical Fourier, SPL and DPL Heat Transfer Model in Biological Tissues in Presence of Metabolic and External heat source, 2015.
- [13] S.-M. Lin, C.-Y. Li, Analytical solutions of non-Fourier bio-heat conductions for skin subjected to pulsed laser heating, *International Journal of Thermal Sciences*, 110 (2016) 146-158.
- [14] J. Ma, X. Yang, S. Liu, Y. Sun, J. Yang, Exact solution of thermal response in a three-dimensional living bio-tissue subjected to a scanning laser beam, *International Journal of Heat and Mass Transfer*, 124 (2018) 1107-1116.
- [15] A. Welch, The thermal response of laser irradiated tissue, *IEEE Journal of Quantum Electronics*, 20(12) (1984) 1471-1481.
- [16] D. Germain, P. Chevallier, A. Laurent, M. Savart, M. Wassef, H. Saint-Jalmes, MR monitoring of laser-induced lesions of the liver in vivo in a low-field open magnet: Temperature mapping and lesion size prediction, 2001.
- [17] S. Soni, H. Tyagi, R.A. Taylor, A. Kumar, Investigation on nanoparticle distribution for thermal ablation of a tumour subjected to nanoparticle assisted thermal therapy, *Journal of thermal biology*, 43 (2014) 70-80.
- [18] R. Van Hillegersberg, J.W. Pickering, M. Aalders, J.F. Beek, Optical properties of rat liver and tumor at 633 nm and 1064 nm: photofrin enhances scattering, *Lasers in surgery and medicine*, 13(1) (1993) 31-39.
- [19] C. Li, J. Miao, K. Yang, X. Guo, J. Tu, P. Huang, D. Zhang, Fourier and non-Fourier bio-heat transfer models to predict ex vivo temperature response to focused ultrasound heating, 2018.

#### HOW TO CITE THIS ARTICLE

M.Balavand, I.Eltejaei, A.Mojra, A numerical approach to non-Fourier heat transfer in liver tumor during laser irradiation, *AUT J. Model. Simul.*, 52(2) (2020) 259-268.

DOI: [10.22060/miscj.2020.18437.5212](https://doi.org/10.22060/miscj.2020.18437.5212)



